

Anomalous accumulation rates in the Vostok ice-core resulting from ice flow over Lake Vostok

Katherine Leonard, Robin E. Bell, Michael Studinger, and Bruno Tremblay

Lamont-Doherty Earth Observatory of Columbia University, Palisades, New York, USA

Received 24 July 2004; revised 8 October 2004; accepted 10 November 2004; published 17 December 2004.

INDEX TERMS: 1827 Hydrology: Glaciology (1863); 4540 Oceanography: Physical: Ice mechanics and air/sea/ice exchange processes; 9310 Information Related to Geographic Region: Antarctica. **Citation:** Leonard, K., R. E. Bell, M. Studinger, and B. Tremblay (2004), Anomalous accumulation rates in the Vostok ice-core resulting from ice flow over Lake Vostok, *Geophys. Res. Lett.*, 31, L24401, doi:10.1029/2004GL021102.

[1] The accumulation rate of snow is crucial to the development of accurate age-depth models for ice-cores. The dating of the Vostok ice-core assumes that accumulation rates generally vary linearly between the core site and the ice divide 250 km to the west [Jouzel *et al.*, 1996; Lorius *et al.*, 1985; Petit *et al.*, 1999], an assumption which impacts the timing of prominent climatic transitions. We present evidence for a local accumulation rate anomaly at the ice surface above the western shoreline of Lake Vostok. A significant thickening between isochronous layers results from this geographically fixed high accumulation zone which can be stratigraphically traced to a depth of 820–1100 m in the Vostok ice-core, a portion known for its high accumulation rates and paleoclimate records that deviate from other Antarctic ice-core records. This non-climatic accumulation anomaly in the Vostok ice-core impacts the flow dependent age models and subsequent interpretations of sequencing of global climate shifts during the last glacial. Additional unrecognized accumulation anomalies are likely present at other depths in this and other cores. These previously unreported geographically fixed accumulation rate anomalies are introduced into ice-cores drilled away from ice domes (e.g., Byrd and Vostok) and should be considered in age depth models.

[2] The Vostok ice-core, well known for its paleoclimate record [Petit *et al.*, 1999], was drilled over Lake Vostok, a large subglacial lake located in central East Antarctica [Kapitsa *et al.*, 1996] (Figure 1). Ice-penetrating radar profiles collected over Lake Vostok on a regular grid (spaced 7.5 km by 11.25–22.5 km) contain bright continuous internal reflectors to depths of 3 km below the ice surface [Bell *et al.*, 2002; Studinger *et al.*, 2003]. These internal reflectors (Figure 2a) are isochronous layers that formed at the surface and have been advected to their current depths by ice flow while new snow accumulates at the surface [Paren and Robin, 1975; Robin, 1983]. We traced these layers to the Vostok core site [Siebert *et al.*, 1998] and inferred their ages from the Vostok age-depth model [Petit *et al.*, 1999]. As the ice flows over the lake, the layers sag 100–400 m at the lake edge. Downstream, the

younger layers (Figure 2a) gradually slope upwards to the east where a distinct hinge point or change in slope marks their return to their original elevation. Deeper isochrons parallel the lake surface and do not follow this pattern, thus we believe it is a function of surface accumulation rather than freeze-on at the bed. At increased depths, these hinge points are found at increased distances from the shoreline (Figure 2a (middle)).

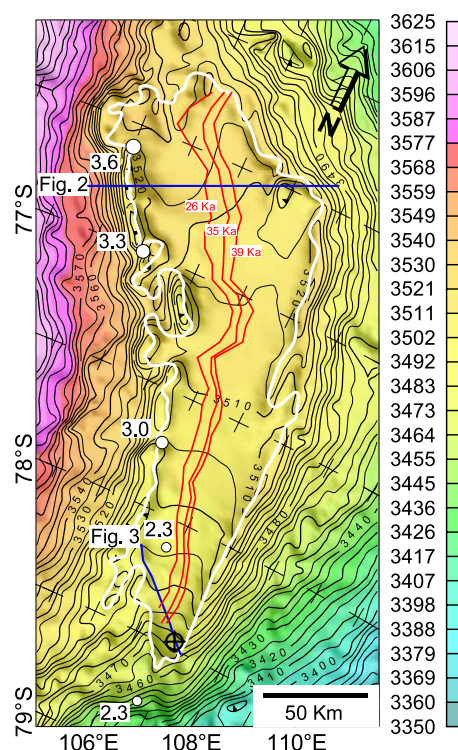


Figure 1. Ice surface elevation over Lake Vostok in m above sea level [Studinger *et al.*, 2003]. Contour interval is 5 m. The solid white line marks the grounding line between the flat, featureless ice over the lake and the rough ice surface over the grounded ice sheet. The ice flow over the lake is primarily from west to east, with a southward component over the southern end of the lake. The slope of the grounded ice surface is relatively steep at the western shoreline and becomes very flat over the lake. The Vostok ice-core site is marked by the blue compass symbol at the southeastern edge of the lake. The locations of profiles shown in Figures 2 and 3 are indicated by solid blue lines. White circles are locations with magnitude labels of surface accumulation rate measurements in $\text{g cm}^{-2} \text{yr}^{-1}$ [Dahe *et al.*, 1994]. The hinge lines (see text) for 26, 35, and 39 kyr BP are plotted in red over the lake.

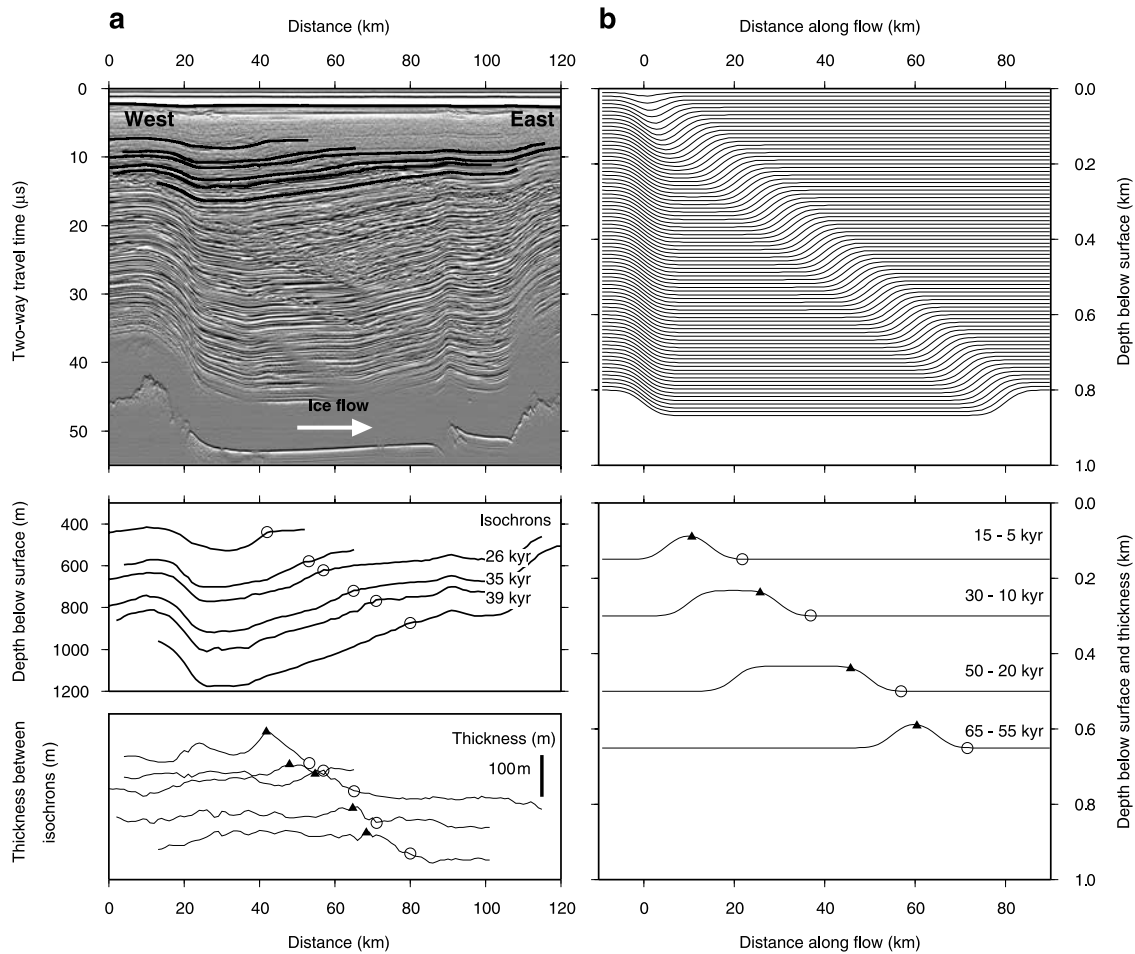


Figure 2. a) (top) Airborne ice-penetrating radar profile parallel to the ice flow. For location see Figure 1. The bright horizontal reflector at the bottom is the lake reflector. The internal layers (black lines) sag into the lake on the west as the ice sheet flows over the lake. (middle) The hinge point locations for six isochronous layers where the shallow internal layers gradually return to their initial elevation are marked by open circles. (bottom) Stacked isopachs calculated from the six internal layers shown in the middle panel. The hinge points are indicated by open circles, as the onset of thickening in the isopachs. The eastern edges of the thickened isopachs are noted as closed triangles. b) (top) Modelled isochrons (1 kyr intervals) between the present and 80 kyr BP for accumulation rates and ice flow velocities typical for the profile shown in a). (bottom) Stacked isopachs from this deposition model calculated with varying time intervals between the isochrons. The shoulder of the maximum thickness and the hinge points are marked as in Figure 2a. Note that the maximum amplitude of the thickened interval is time-independent.

[3] Identifying the hinge points on east-west radar profiles spaced every 7.5 km enables us to locate each hinge line over the entire lake (Figure 1, map view). The hinge line for each layer (26, 35, and 39 kyr before present, BP) resembles the western shoreline of the lake with a prominent bulge occurring downstream of the major peninsula at 77.3°S. The age and depth of the hinge lines increases downflow, to the east.

[4] At shallow depths (<1200 m), a change in thickness between two layers is associated with each hinge line. Isopachs, the thickness of ice between two layers, reveal 40–60 m localized thickening upflow (west) of the hinge line (Figure 2a (bottom)). The bulge within the isopachs is consistently thicker by 40–60 m and its width broadens with increasing age difference between the bounding layers (Figure 2a (bottom)). Similar to the hinge lines, the eastern edges of the bulges are identified at greater depths downflow (east). These bulges may be due either to deformation

associated with ice sheet motion, or to a spatially fixed localized surface accumulation anomaly at the time of deposition [Jacobel *et al.*, 1993; Nereson *et al.*, 2000; Vaughan *et al.*, 1999]. The location of the thickened deposits near the ice surface (i.e., far removed from basal stresses) and the fact that the shape of the hinge lines resembles the western shoreline advected downstream along flow trajectories [Bell *et al.*, 2002; Tikku *et al.*, 2004], are evidence that the thickened deposits result from surface processes and not deformation. Additional evidence for accumulation rather than deformation as the cause of these features is the fact that they are only present near the ice surface.

[5] The western shoreline is a region of localized high accumulation. Shallow cores [Dahe *et al.*, 1994] along the western shoreline document elevated accumulation rates (Figure 1). Within this region the ice surface is marked by a distinct change in surface slope (Figure 1) that could lead

to enhanced aeolian deposition of katabatic wind-blown snow, creating a localized region of high accumulation [Anderson and Hallet, 1986; Bagnold, 1954]. The regional gradient in surface elevation upflow (west) of the lake is roughly 1 m km^{-1} sloping down towards the lake. Over the lake, the surface slope of the ice is less than 0.3 m km^{-1} along-flow. In between, at the western shoreline, the surface slope is as high as $8\text{--}10 \text{ m km}^{-1}$ over a distance of less than 5 km along-flow. As this snow transforms into ice, the increased accumulation signal is preserved within the ice sheet as a shoreline – parallel band of thickened ice. Because the increased accumulation remains at a fixed geographic location on top of a moving ice sheet, the thickened deposits are advected down and to the east over time (Figure 2). The hinge marks the downstream edge of the thickened deposit and the eastern edge of the bulge is found upstream of the hinge line.

[6] The geometry of the thickened deposits provides new insights into regional accumulation rates and local ice sheet paleo-velocities. Using the dates determined from the Vostok ice-core, we calculated the average accumulation rate for four isopach intervals by dividing the isopach thickness by the age difference of its bounding layers. The thickened deposits yield high accumulation rates of $>2 \text{ cm yr}^{-1}$ of ice equivalent. Ice downflow (east) of the thickened deposits formed over Lake Vostok is characterized by low and extremely regular accumulation rates of $\sim 1 \text{ cm yr}^{-1}$ (Figure 2a (bottom)) while the upstream ice formed to the west of Lake Vostok is characterized by highly variable patchy accumulation (with an average of 1.2 cm yr^{-1} and a 1 cm yr^{-1} standard deviation). Along two flow lines (Figure 1), the distance between the dated hinge points can be used to calculate the past ice sheet velocity [Ng and Conway, 2004]. In the north, between 26–39 kyr BP the ice sheet's velocity was 1 m yr^{-1} . Along the southern flow line, intersecting the Vostok ice-core, the velocity for the same time interval is 0.7 m yr^{-1} . These rates are significantly lower than the present day velocities of $\sim 2.0 \text{ m yr}^{-1}$ determined from GPS positioning (R. Dietrich, personal communication), as would be projected by the substantially lower accumulation rates of ice in the past.

[7] We developed a 2-dimensional model of snow/ice accumulation and advection that reproduces key characteristics of the observed layer geometry and isopach thickening. Our simple geometric model applies only to the floating portion of the ice sheet, as we do not vary velocity either laterally or vertically. In this model, a bell-shape surface snow-accumulation rate curve of width w (m) and amplitude h (m yr^{-1}), accumulates onto an ice sheet moving at speed u (m yr^{-1}). The depth and geometry of the simulated layers were obtained by summing the accumulation curve each year while displacing the underlying ice sheet downflow by u meters every year (Figure 2b). Using the calculated background accumulation rate (1 cm yr^{-1}) and paleo-velocity (1 m yr^{-1}) for the northern profile, a 16-km-wide increased-accumulation zone of amplitude 1 cm yr^{-1} at the western shoreline will produce the layer geometry and accumulation anomaly (Figure 2b) observed in the radar data (Figure 2a). The stratigraphy for this configuration predicts layers which sag below the fixed high accumulation point and return to their original depth downstream. The

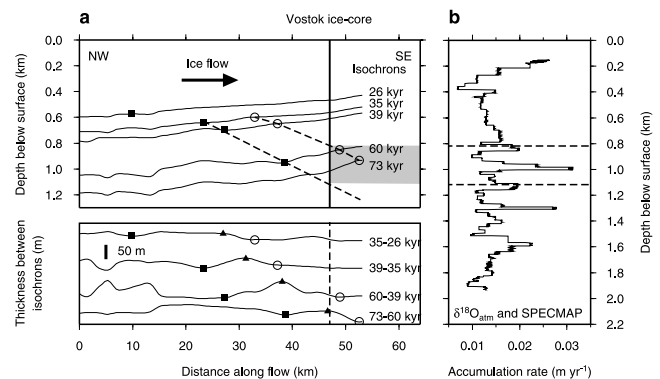


Figure 3. a) Stacked isochrons (top) and isopach thickness interpolated along the Vostok ice core flow line from gridded depth maps. For location see Figure 1. The hinge points (open circles) are indicated as the change in slope of the isochrons (top) and as the onset of thickening in the isopachs (bottom). The shoulder of the maximum thickness of the isopachs is noted as a closed triangle. Closed squares mark the locations of trailing edges. The projection of the hinge points (open circles) and the trailing edges (closed squares) into the Vostok ice-core are marked by dashed lines. The depth interval in which the Vostok ice-core is influenced by the high accumulation rates along the western shoreline is highlighted by the grey area. b) Accumulation rates calculated from correlating $\delta^{18}\text{O}_{\text{atm}}$ with $\delta^{18}\text{O}_{\text{sw}}$ and the SPECMAP timescale [Sowers *et al.*, 1993]. The ice deposited in the shoreline region with anomalously high accumulation rates is marked by dashed lines.

well-defined hinges and bulges migrate down and to the east with age. In the simulated layer the hinges are clearly resolved as the points where thickening begins (Figure 2b (bottom), open circles). The bulges within the isopachs are characterized by a maximum thickness of 60 m at the eastern edge (Figure 2b (bottom), triangles). The lateral extent of the thickened deposit depends on the age difference between the layers.

[8] To identify the depth range within the Vostok ice-core impacted by this localized surface high accumulation zone, we extracted the depth of five internal layers along the Vostok flow line (Figure 3a). We calculated four isopachs along this profile from which the hinge points are identified (Figure 3a, open circles). Upflow of the hinge points, the isopachs are thickened by 15–50 m (triangles). The trailing edge of the thickened deposit is marked as a square (Figure 3a). The projection of the hinge and the trailing edge of thickened isopachs along the Vostok flow line intersect the ice-core site at 820 m and 1100 m depth respectively ($\pm 30 \text{ m}$). This observed 280 m thick impacted interval is close to our model prediction of a 250 m thick interval using accumulation characteristics and ice velocity typical of the Vostok trajectory.

[9] In this segment of the Vostok ice-core (820–1100 m) the age-depth models diverge significantly. For example, Jouzel *et al.* [Jouzel *et al.*, 1993] estimate the age of this 280 m thick interval to be 53.7–77.59 kyr while Sowers *et al.* [Sowers *et al.*, 1993] estimate the age to be 56.5–75.2 kyr. The timing of the Vostok climate record also diverges from other Antarctic ice cores (Figure 4). Our

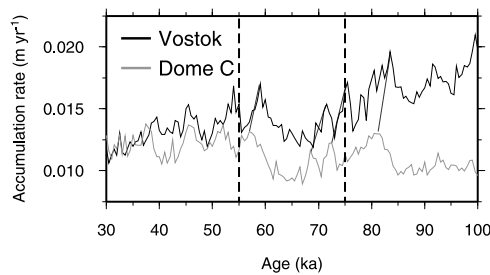


Figure 4. Accumulation rates from Vostok [Parrenin *et al.*, 2004] and Dome C [EPICA Community Members, 2004] between 30,000 and 100,000 years ago. Dashed vertical lines mark the interval of the Vostok core impacted by the accumulation anomaly. Solid straight lines demonstrate the offset between astronomically forced peaks in accumulation at these two sites. The Vostok record lags the Dome C record due to anomalous accumulation rates which were not incorporated into the Vostok age model.

modelling of the Vostok trajectory necessitates a 56% increase in the surface accumulation rate suggesting the 300 m of impacted ice represents a time interval of 19 kyr. Calculating accumulation rates by correlating $\delta^{18}\text{O}$ of atmospheric O_2 ($\delta^{18}\text{O}_{\text{atm}}$) with $\delta^{18}\text{O}$ of sea water ($\delta^{18}\text{O}_{\text{sw}}$) and the SPECMAP timescale [Sowers *et al.*, 1993] between 820–1100 m produces values as large as 2–3 cm yr^{-1} (Figure 3b), similar in amplitude to our model prediction.

[10] Subglacial lakes such as Lake Vostok can produce spatially fixed changes in surface slope that can produce significant localized anomalies in the accumulation record. The stratigraphic manifestation of the localized shoreline accumulation zone is clearly preserved due to the absence of basal stress over Lake Vostok. Evidence for additional deeper accumulation anomalies includes similar disruption of isochronous layers with increasing depth downflow and the presence of persistent thickening of isopachs to the west of the shoreline deposit described here. These results suggest that other accumulation anomalies associated with fixed subglacial topographic features are likely present within Vostok and other ice-cores but are rarely recognized. The anomalous accumulation rates produced by such topography will impact the age models at greater depths, and must be considered in the interpretation of the phasing of global climatic records.

[11] **Acknowledgments.** Helpful comments by R. Alley, R. Bindshadler, G. Clarke, H. Fischer, R. Jacobel and F. Parrenin improved this manuscript. Radar internal layer picking by J. Laatsch and A. Tikku, is gratefully acknowledged. U. S. National Science Foundation grants OPP99-78236, OPP00-88047 and OPP98-18711 funded this work. F. Parrenin's

generous assistance in providing new data is gratefully acknowledged. LDEO Contribution Number 6673.

References

- Anderson, R. S., and B. Hallet (1986), Sediment transport by wind: Toward a general model, *Geol. Soc. Am. Bull.*, **97**, 523–535.
- Bagnold, R. A. (1954), *The Physics of Blown Sand and Desert Dunes*, CRC Press, Boca Raton, Fla.
- Bell, R. E., M. Studinger, A. A. Tikku, G. K. C. Clarke, M. M. Gutner, and C. Meertens (2002), Origin and fate of Lake Vostok water frozen to the base of the East Antarctic ice sheet, *Nature*, **416**, 307–310.
- Dahe, Q., J. R. Petit, J. Jouzel, and M. Stievenard (1994), Distribution of stable isotopes in surface snow along the route of the 1990 International Trans-Antarctic Expedition, *J. Glaciol.*, **40**, 107–118.
- EPICA Community Members (2004), Eight glacial cycles from an Antarctic ice core, *Nature*, **429**, 623–628.
- Jacobel, R. W., A. M. Gades, D. L. Gottschling, S. M. Hodge, and D. L. Wright (1993), Interpretation of radar-detected internal layer folding in West Antarctic ice streams, *J. Glaciol.*, **39**, 528–537.
- Jouzel, J., *et al.* (1993), Extending the Vostok ice-core record of palaeoclimate to the penultimate glacial period, *Nature*, **364**, 407–412.
- Jouzel, J., *et al.* (1996), Climatic interpretation of the recently extended Vostok ice records, *Clim. Dyn.*, **12**, 513–521.
- Kapitsa, A. P., J. K. Ridley, G. d. Q. Robin, M. J. Siegert, and I. A. Zotikov (1996), A large freshwater lake beneath the ice of central East Antarctica, *Nature*, **381**, 684–686.
- Lorius, C., J. Jouzel, C. Ritz, L. Merlivat, N. I. Barkov, Y. S. Korotkevich, and V. M. Kotlyakov (1985), A 150,000-year climatic record from Antarctic ice, *Nature*, **316**, 591–596.
- Nereson, N. A., C. F. Raymond, R. W. Jacobel, and E. D. Waddington (2000), The accumulation pattern across Siple Dome, West Antarctica, inferred from radar-detected internal layers, *J. Glaciol.*, **46**, 75–87.
- Ng, F., and H. Conway (2004), Fast-flow signature in the stagnated Kamb Ice Stream, West Antarctica, *Geology*, **32**, 481–484.
- Parrenin, F., G. d. Q. Robin (1975), Internal reflections in polar ice sheets, *J. Glaciol.*, **14**, 251–259.
- Parrenin, F., F. Rémy, C. Ritz, M. J. Siegert, and J. Jouzel (2004), New modeling of the Vostok ice flow line and implication for the glaciological chronology of the Vostok ice core, *J. Geophys. Res.*, **109**, D20102, doi:10.1029/2004JD004561.
- Petit, J. R., *et al.* (1999), Climate and atmospheric history of the past 420,000 years from the Vostok ice core, Antarctica, *Nature*, **399**, 429–436.
- Robin, G. d. Q. (1983), *The Climatic Record in Polar Ice Sheets*, Cambridge Univ. Press, New York.
- Siegert, M. J., R. Hodgkins, and J. A. Dowdeswell (1998), Internal radio-echo layering at Vostok station, Antarctica, as an independent stratigraphic control on the ice-core record, *Ann. Glaciol.*, **27**, 360–364.
- Sowers, T., M. Bender, L. Labeyrie, D. Martinson, J. Jouzel, D. Raynaud, J. J. Pichon, and Y. S. Korotkevich (1993), A 135,000-year Vostok-SPECMAP common temporal framework, *Palaeoceanography*, **8**, 737–766.
- Studinger, M., *et al.* (2003), Ice cover, landscape setting, and geological framework of Lake Vostok, East Antarctica, *Earth Planet. Sci. Lett.*, **205**, 195–210.
- Tikku, A. A., R. E. Bell, M. Studinger, and G. K. C. Clarke (2004), Ice flow over Lake Vostok, East Antarctica inferred by structure tracking, *Earth Planet. Sci. Lett.*, **227**, 249–261.
- Vaughan, D. G., H. F. J. Corr, C. S. M. Doake, and E. D. Waddington (1999), Distortion of isochronous layers in ice revealed by ground-penetrating radar, *Nature*, **398**, 323–326.

R. E. Bell, K. Leonard, M. Studinger, and B. Tremblay, Lamont-Doherty Earth Observatory of Columbia University, 61 Route 9W, Palisades, NY 10964, USA. (kleonard@ldeo.columbia.edu)